Journal of Non-Crystalline Solids 437 (2016) 6–9

Contents lists available at ScienceDirect

Journal of Non-Crystalline Solids

journal homepage: www.elsevier.com/locate/jnoncrysol

Pressure-induced phase transformations in amorphous arsenic

Murat Durandurdu

Department of Materials Science & Nanotechnology Engineering, Abdullah Gül University, Kayseri 38080, Turkey

ARTICLE INFO

Article history:
Received 9 October 2015
Received in revised form 13 December 2015
Accepted 20 January 2016
Available online 28 January 2016

Keywords:
Arsenic
Polyamorphism
Amorphous-to-amorphous
Pressure
Crystallization

ABSTRACT

The atomic structure of amorphous arsenic and its response to high pressure are explored using a constant pressure ab initio molecular dynamics technique. Different analyzing techniques reveal that amorphous arsenic has a local structure close to that of the crystalline phase. The model also presents some twofold and fourfold coordination defects. The existence of a possible amorphous to amorphous phase transition for arsenic is proposed on the bases of the observation of a gradual coordination increase with the application of pressure. Further compression of the amorphous state yields a transformation into a simple cubic crystal.

1. Introduction

Arsenic (As) is one of the group-V elements with some interests. Its ground state is the rhombohedral A7 structure with covalent bonding. The A7 crystal has three nearest (intralayer) and three next (interlayer) neighbors and can be considered as a layer like structure. The A7 phase can be originated from a Peierls distorted simple cubic (SC) structure by a rhombohedral shear distortion along the [111] direction and an internal displacement of (111) planes toward each other in pairs along the [111] (Ref. [1]). The lowering symmetry from the SC phase to the rhombohedral A7 structure strongly reduces the electronic states near the Fermi level and a metal-to-semimetal transition is observed.

Amorphous form of arsenic (*a*-As) exists as well. It was investigated extensively in the past and valuable information regarding its atomic structure and physical properties was revealed in these studies [2–25]. Yet its response to high-pressure has been prompted in limited experiments so far. One experiment [21] stated a structural phase transition from an amorphous phase to an A7 structure at 4.0 kbar while the other [22] focused on simply the influence of pressure to the optical properties of *a*-As. Consequently, the high pressure behavior of *a*-As remains an open problem in solid state physics and materials science.

Both experimental and theoretical analyses [26–34] have shown an interesting phenomenon in some amorphous materials subjected to high pressure, viz. they undergo an amorphous-to-amorphous phase transformation, which is referred as polyamorphism [26] and indicates the distinct amorphous states having different density and bonding environments. Does such a phase transition occur in *a*-As as well? The main purpose of the present work is to find an answer to this question using a constant pressure molecular dynamics (MD) technique. Based on the results obtained through the MD simulations, the presence of amorphous-to-amorphous and amorphous-to-crystalline phase transformations is suggested for *a*-As.

2. Computational technique

The MD simulations were achieved by means of SIESTA ab initio code [35] based on the density functional theory (DFT) and a localized linear combination of atomic orbitals as basis sets. We used the Troullier and Martins approach to construct norm-conserving pseudopotential [36]. The exchange correlation energy was calculated by the generalized gradient approximation of PBE [37]. We adopted the double-ξ plus polarized basis set and Γ point sampling for the Brillouin zone integration for the calculations. The MD simulations were carried out using the NPT (constant number of atoms, constant pressure, and constant temperature) ensemble. One femtosecond (fs) was used for each MD time step. A randomly distributed disordered network having 160 atoms was chosen as a starting structure with the periodic boundary conditions. The initial random structure was subjected to a high temperature of 1150 K for 45.0 ps and its volume was adjusted by the Parrinello–Rahman method [38] but shear deformations were not allowed. The liquid state was cooled to 300 K in a period of 65.0 ps. The external pressure was increased gradually by an increment of 2.5 GPa. At each applied pressure, the amorphous model at 300 K was equilibrated for at least 15.0 ps. Temperature was controlled using the velocity rescaling

E-mail address: murat.durandurdu@agu.edu.tr.

http://dx.doi.org/10.1016/j.jnoncrysol.2016.01.014
0022-3093/

method [39]. In order to visualize the structure, the VESTA program [40] was applied.

3. Results

The pair distribution function (PDF) provided in Fig. 1 allows us at some level to have an atomistic level description of *a*-As and to understand the impact of pressure on its local structural arrangements. At zero pressure, the first, second and third neighbor separations are located at 2.56 Å, 3.97 Å and 5.74 Å, respectively which are fairly close to the experimental results of 2.49 Å (X-ray) [23], 2.51 Å (neutron) [24], 3.78 Å (X-ray and neuron) [23,24] and 5.76 Å (X-ray) [23]. The minima in the PDF at 2.88 Å and 4.55 Å are also comparable with 2.9 Å and 4.6 Å reported in the X-ray study [23]. It should be noted here that the first peak position further accords with the first neighbor separations of 2.52 Å and 2.54 Å reported for the rhombohedral A7 crystal and liquid As [41], respectively. All these findings offer that our model fairly represents the atomic structure of *a*-As.

When the model is subjected to high pressure, the first peak position, as illustrated in Fig. 2, exhibits a quite complex behavior: generally it has a tendency to decrease under pressure but at some pressures it rapidly increases to a higher value. A close evaluation of the structure demonstrates that the abrupt change in the position is a result of the noticeable coordination increase at these pressures (see below). The behavior of the first peak position of *a*-As under pressure appears to be quite different from that of the compressed liquid and crystalline As [41]. Namely in the liquid state, the position of the first peak increases gradually and reaches almost a constant value above 10 GPa while in the crystal it uniformly decreases until the A7-to-SC phase change occurs at 35 GPa [41]. Consequently, *a*-As acts like a mixture of these two states when the trend of the first neighbor separation under pressure is considered. The PDF investigation and the visualization of the model (see Fig. 3) reveal that the system remains amorphous with some crystalline portions (SC type structure) at 25 GPa and it fully transforms to a crystalline phase as indicated by the appearance of pronounced peaks at long-range correlations at 27.5 GPa. As seen from Fig. 3, the crystal at 27.5 GPa has a SC structure having some distortions and structural defects.

The atomic structure of *a*-As and its response to the external pressure are additionally evaluated by the bond angle distribution function that is given in Fig. 4. At zero pressure, the distribution has a main peak around 97°, offering supportive evidence that *a*-As has a local environment similar to that of the A7 crystal. The large angles presented in the model are due to the twofold coordinated chain-like structures. With increasing pressure, the main peak gradually shifts toward to 90° and more large angles appear in the distribution, suggesting that the system has a tendency to form the octahedral-like configurations. At 27.5 GPa, the distribution has two main peaks around 90° and 180° as presented in a SC structure. The splitting of the peak near 90° is due to the distortion of the SC crystal.

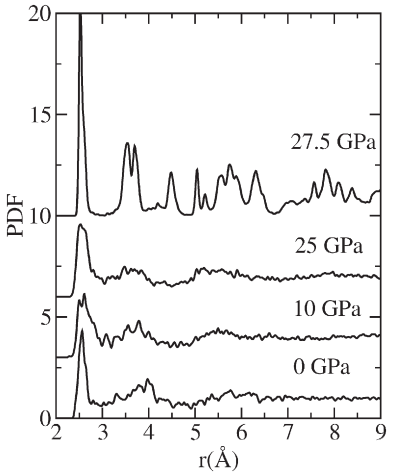

Fig. 1. Pair distribution function (PDF) at different pressures.

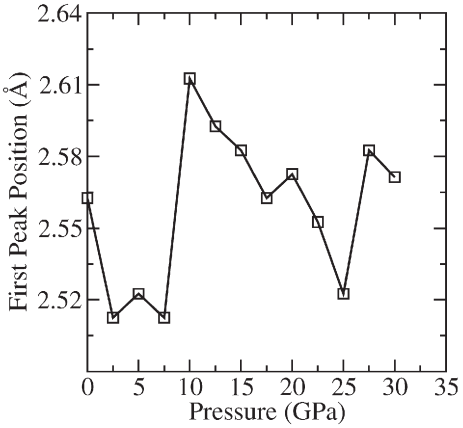

Fig. 2. Variation of the first neighbor separation as a function of pressure.

The coordination number (CN) is a principal physical parameter and the pressure-induced phase transitions of materials are frequently identified by it. The average CN change and the coordination distributions as a function of pressure are shown in Fig. 5. At zero-pressure, 81% of atoms are found to be threefold coordinated. The fraction of the twofold and fourfold coordinated atoms is roughly 10% and 9% respectively. These fractions lead to an average CN of 2.97 at zero-pressure, which is reasonably close to that of the A7 crystal. As understood from Fig. 5, the CN of *a*-As is very sensitive to pressure and increases progressively with increasing pressure. Yet in some pressure regions (between 7.5 and 12.5 GPa) or at a pressure (27.5 GPa), the change is quite drastic. At 10 GPa the fourfold coordination becomes dominated. Further increase in pressure results into more fivefold and sixfold coordinated clusters As expected the system has mostly the sixfold configurations at 27.5 GPa.

In order to better understand the structural rearrangements in the short-range order under pressure and to find connections between the high-pressure amorphous state and the crystalline forms of As, it is essential to describe the geometry of the high coordinated clusters

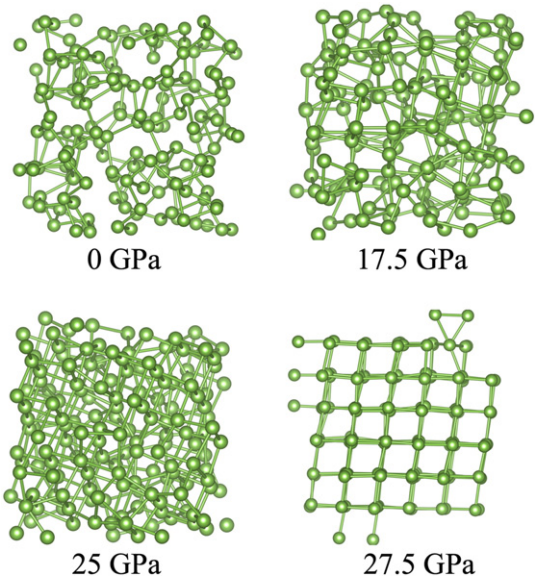

Fig. 3. Ball stick representation of arsenic obtained through the MD simulations at different pressures.

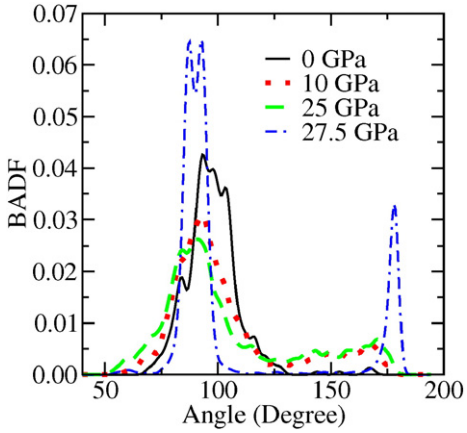

Fig. 4. Bond angle distribution function at different pressures.

formed in the amorphous system. The sixfold-coordinated configurations are octahedrons (see Fig. 6). On the other hand, the fivefold-coordinated units have a central atom surrounded by five atoms and can be considered as a square based pyramidal geometry. Therefore they are the incomplete octahedrons with missing one of the atoms on the plane passing through the top vertex and perpendicular to the base of the pyramid. The fourfold-coordinated configurations are the imperfect square pyramids with missing one of the atoms on the base of the pyramid. All these observations imply a close topological similarity between the high-pressure amorphous phase and the SC structure.

4. Discussion

All structural analyses offer strong evidences that the short-range order of *a*-As is quite close to that of the A7 crystal. Yet the model presents twofold and fourfold coordination defects. The existence of both types of defects (without providing their fraction) in *a*-As was discussed in the Raman study [42]. Therefore our finding agrees with the experiment [42]. Yet about 20% coordination defects predicted in the simulation are indeed quite large but there is no experimental evidence in the Literature to support or dispute our prediction. It is likely that the high fraction is due to the simulation conditions (finite size effect, time scale etc.).

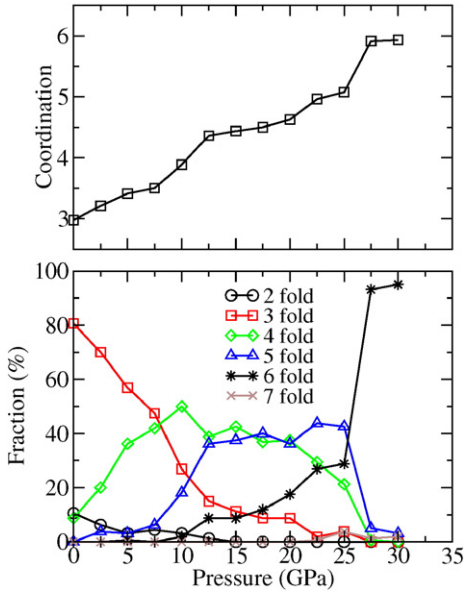

Fig. 5. Average coordination number and coordination distribution as a function of pressure.

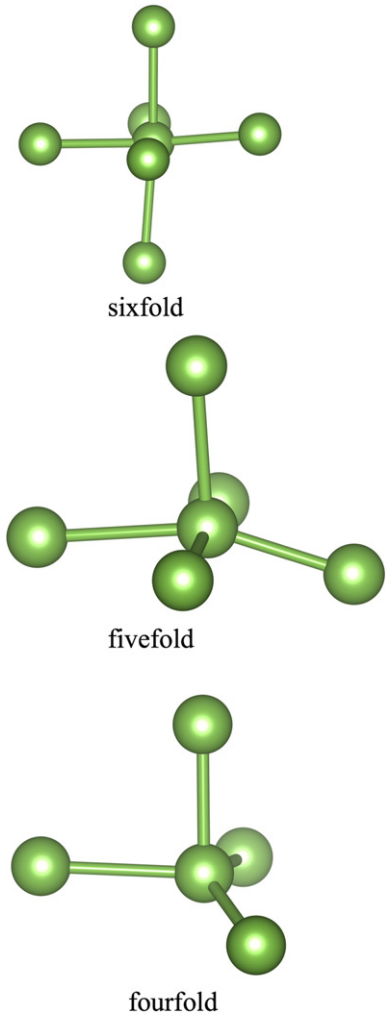

Fig. 6. High coordinated clusters formed in arsenic obtained through the MD simulations at high pressure.

Based on the variation of the average CN under pressure, we speculate that the low density amorphous state persists at low pressure regimes and the transformation to the high-density amorphous phase occurs between at 7.5 GPa and at 12.5 GPa. However, a very high-density amorphous phase having a CN of about six does not exist since *a*-As has a tendency to crystallize into a SC structure. The four and fivefold coordinated atoms are the main building blocks of the high-density amorphous phase.

The nature of amorphous-to-amorphous phase transformations is of interest. The transformation can be first order such that the CN drastically changes and the volume exhibits a large drop or can be gradual without showing a sharp volume collapse. Although the modification of the average CN suggests a gradual phase transition for *a*-As, we plot the pressure–volume relation in Fig. 7 to confirm this suggestion. As can be seen from the figure, the volume varies quite smoothly without presenting a very sharp decrease in spite of a noticeable CN modification in some pressure ranges or a certain pressure. This finding is indeed unsurprising because the A7-to-SC phase transition is also accompanied by no volume modification [1] or a 5% volume reduction even though the CN changes from three to six. A carefully analysis suggests that the crystallization indeed starts around at 17.5 GPa (see Fig. 3) and completes at 27.5 GPa and hence the amorphous-to-crystalline phase transformation can be considered as a relaxation phenomena.

Finally we would like to point out here that the transition pressures predicted in our simulations are overestimated. This is a well-known limitation of the Parrinello–Rahman approach [43] and can be

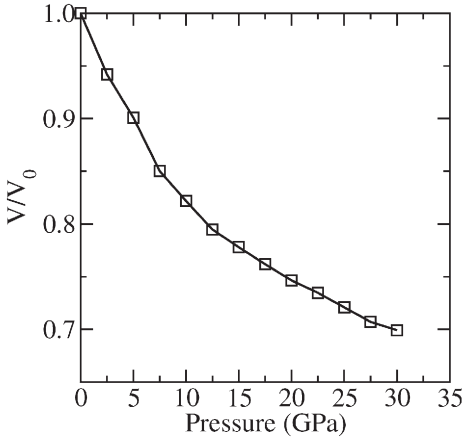

Fig. 7. Pressure–volume relation.

attributed to the simulation conditions such as lack of surface effects because of the use of periodic boundary condition, time scale of the MD simulation etc. Therefore, the phase transformations are anticipated to take place at lower pressures in experiments.

5. Conclusions

We report the microscopic structure of *a*-As and its high-pressure behavior by means of constant pressure ab initio MD simulations. The model is dominantly threefold coordinated and has a short-range order similar to that of the crystalline As. It also presents the twofold and fourfold coordination defects. With the application of pressure, the average CN increases progressively and a high-density amorphous phase forms up to the molecular dynamic pressure of 27.5 GPa at which point it crystallizes into a SC structure. Based on these findings, we propose the presence of a gradual amorphous-to-amorphous phase transitions in *a*-As.

Acknowledgement

This work was supported by the Abdullah Gül University Support Foundation.

References

[1] H.J. Beister, K. Strössner, K. Syassen, Rhombohedral to simple-cubic phase transition in arsenic under pressure, Phys. Rev. B 41 (9) (1990) 5535.
[2] W.B. Pollard, J.D. Joannopoulos, Electronic structure of defects in amorphous arsenic, Phys. Rev. B 19 (8) (1979) 4217.
[3] E.A. Davis, E. Mytilineou, Chemical modification of amorphous arsenic, Sol. Energy Mater. 8.1 (1982) 341–348.
[4] E.A. Davis, et al., Phonons in amorphous and rhombohedral arsenic, J. Non-Cryst. Solids 32 (1) (1979) 257–270.
[5] G.N. Greaves, S.R. Elliott, E.A. Davis, Amorphous arsenic, Adv. Phys. 28 (1) (1979) 49–141.
[6] D.P. Jones, N. Thomas, W.A. Phillips, The low-temperature thermal properties of amorphous arsenic, Philos. Mag. B 38 (3) (1978) 271–288.
[7] M.J. Kelly, D.W. Bullett, Calculation of the electronic structure of crystalline and amorphous arsenic, Solid State Commun. 18 (5) (1976) 593–595.
[8] M.P. Brassington, et al., The second- and third-order elastic constants of amorphous arsenic, Philos. Mag. B 42 (1) (1980) 127–148.
[9] A.J. Leadbetter, P.M. Smith, P. Seyfert, Vibrational properties of amorphous and two crystalline modifications of arsenic as determined by inelastic neutron scattering, Philos. Mag. 33 (3) (1976) 441–456.
[10] G.N. Greaves, E.A. Davis, J. Bordas, Optical properties of amorphous arsenic, Philos. Mag. 34 (2) (1976) 265–290.
[11] J.C. Knights, J.E. Mahan, Optical and electrical properties of amorphous arsenic, Solid State Commun. 21 (10) (1977) 983–986.
[12] J. Knights, Localized states in amorphous arsenic, Solid State Commun. 16 (5) (1975) 515–519.
[13] J.S. Lannin, H.F. Eno, H.L. Luo, The specific heat of bulk amorphous arsenic, Solid State Commun. 25 (2) (1978) 81–84.
[14] G. Breitling, Different forms of amorphous arsenic and germanium, J. Non-Cryst. Solids 8 (1972) 395–400.
[15] P.M. Smith, A.J. Leadbetter, A.J. Apling, The structures of orthorhombic and vitreous arsenic, Philos. Mag. 31 (1) (1975) 57–64.
[16] M.P. Fontana, et al., Temperature dependence of EXAFS in amorphous arsenic, Solid State Commun. 43 (7) (1982) 561–565.
[17] K.S. Gilroy, W.A. Phillips, Ultrasonic attenuation in amorphous arsenic and red phosphorus, J. Non-Cryst. Solids 35 (1980) 1135–1140.
[18] J.S. Lannin, Vibrational properties of amorphous arsenic and antimony, Structure and Excitations of Amorphous Solids, Vol. 31. No. 1, AIP Publishing, 1976.
[19] P.P. Lottici, Phonon and fraction dynamics in amorphous arsenic, Phys. Status Solidi B 146.2 (1988) K81–K85.
[20] M. Popescu, Structural model for amorphous arsenic, Chalcogenide Lett. 2.5 (2005) 45–48.
[21] S.R. Elliot, E.A. Davis, G.D. Pitt, Effect of high pressure on the electrical properties of amorphous arsenic, Solid State Commun. 22 (8) (1977) 481–484.
[22] K. Tanaka, Studies of amorphous arsenic under pressure, Philos. Mag. B 57 (4) (1988) 473–481.
[23] H. Krebs, Electrical conductivity and chemical bonding in crystalline, glassy and liquid phases, J. Non-Cryst. Solids 1 (6) (1969) 455–473.
[24] R. Bellissent, G. Tourand, Étude de l'ordre local dans l'arsenic amorphe par diffraction de neutrons, J. Phys. 37 (12) (1976) 1423–1426.
[25] H. Krebs, R. Steffen, Neubestimmung der nahordnung im glasigen selen, im explosiven antimon und im β-und γ-arsen, Z. Anorg. Allg. Chem. 327 (3–4) (1964) 224–237.
[26] P.H. Poole, et al., Amorphous polymorphism, Comput. Mater. Sci. 4 (4) (1995) 373–382.
[27] O. Mishima, L.D. Calvert, E. Whalley, An apparently first-order transition between two amorphous phases of ice induced by pressure, Nature 314 (6006) (1985) 76–78.
[28] P.F. McMillan, et al., A density-driven phase transition between semiconducting and metallic polyamorphs of silicon, Nat. Mater. 4 (9) (2005) 680–684.
[29] P.F. McMillan, Polyamorphic transformations in liquids and glasses, J. Mater. Chem. 14.10 (2004) 1506–1512.
[30] D.J. Lacks, Localized mechanical instabilities and structural transformations in silica glass under high pressure, Phys. Rev. Lett. 80.24 (1998) 5385.
[31] E. Principi, et al., Pressure induced phase transitions in amorphous Ge, Phys. Scr. 2005.T115 (2005) 381.
[32] L. Huang, J. Kieffer, Amorphous–amorphous transitions in silica glass. I. Reversible transitions and thermomechanical anomalies, Phys. Rev. B 69.22 (2004), 224203.
[33] M. Vaccari, et al., Structural changes in amorphous GeS_2 at high pressure, Phys. Rev. B 81.1 (2010), 014205.
[34] L. Properzi, et al., Short-range order of compressed amorphous $GeSe_2$, Sci. Rep. 5 (2015).
[35] P. Ordejón, E. Artacho, J.M. Soler, Self-consistent order-N density-functional calculations for very large systems, Phys. Rev. B 53 (16) (1996), R10441.
[36] N. Troullier, J.L. Martins, Efficient pseudopotentials for plane-wave calculations, Phys. Rev. B 43.3 (1991) 1993.
[37] J.P. Perdew, K. Burke, M. Ernzerhof, Generalized gradient approximation made simple, Phys. Rev. Lett. 77 (18) (1996) 3865.
[38] M. Parrinello, A. Rahman, Polymorphic transitions in single crystals: a new molecular dynamics method, J. Appl. Phys. 52 (12) (1981) 7182–7190.
[39] W. T. Ashurst, "Dense Fluid Shear Viscosity and Thermal Conductivity via Nonequilibrium Molecular Dynamics" [PhD Dissertation, University of California at Davis/Livermore, 1974].
[40] K. Momma, F. Izumi, VESTA 3 for three-dimensional visualization of crystal, volumetric and morphology data, J. Appl. Crystallogr. 44 (6) (2011) 1272–1276.
[41] A. Chiba, et al., Pressure-induced suppression of the Peierls distortion of liquid As and Ge X (X = S, Se, Te), Phys. Rev. B 80.6 (2009), 060201.
[42] R.J. Nemanich, et al., Spectroscopic evidence for bonding coordination defects in amorphous as, Solid State Commun. 26 (3) (1978) 137–139.
[43] A. Laio, et al., Assessing the accuracy of metadynamics, J. Phys. Chem. B 109 (14) (2005) 6714–6721.